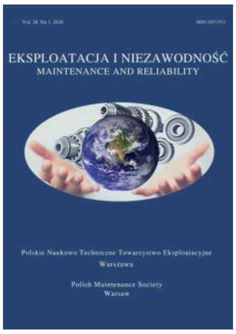

Eksploatacja i Niezawodnosc – Maintenance and Reliability

Volume 28 (2026), Issue 1

journal homepage: http://www.ein.org.pl

Article citation info:
Gonera J, Szymczak T, Analysis of the influence of tyre pressure changes on vehicle operating parameters, Eksploatacja i Niezawodnosc – Maintenance and Reliability 2026: 28(1) http://doi.org/10.17531/ein/209531

Analysis of the influence of tyre pressure changes on vehicle operating parameters

Indexed by: Web of Science Group

Jarosław Krzysztof Gonera[a,*], Tadeusz Szymczak[b]

[a] Department of Vehicles and Machinery, Faculty of Technical Sciences, University of Warmia and Mazury in Olsztyn, Poland
[b] Department of Type Approval and Testing, Motor Transport Institute, Poland

Highlights

- The shock absorber damping coefficient depends on the wheel pressure value;
- There is an influence of the tyre size on the Eusama coefficient value;
- The Digital Image Correlation (DIC) method enables the following behaviour of a wheel;
- There are differences between the displacement values of the wheel due to tyre pressure;
- The influence of wheel pressure on tyre stiffness and operating parameters is described.

Abstract

The paper aimed to identify the effect of changes in tyre pressure values and the influence of wheel size on the shock absorber damping coefficient (EUSAMA coefficient) using 20 passenger cars with SUV bodies. Eleven levels of tyre pressure from 0.10 to 0.30 MPa at 0.02 MPa at its step value equal to 0.02 MPa were used. The component's behaviour was followed through the Digital Image Correlating system PONTOS 5M and measurement markers cemented on a rim, tyre and body. Thanks to this, it was possible to identify the effect of tyre pressure on tyre deformation in a 3D coordinate system and on the vehicle's operating parameters. It was possible to conclude that there is a significant relationship between the values of the shock absorber damping coefficient and the tyre pressure. Moreover, these changes were also dependent on the tyre size. The Eusama coefficient values ranged from about 90% to 60%. At each used pressure value, there were clear differences between the components' behaviour at the region located in the lower and upper part of the tire, as well as between the position of the points in the front and rear part of the tyre concerning the axis of rotation of the wheel. Changes in tyre pressure values on an actual linear vehicle speed value were also covered at the wheel pressure values employed

Keywords

vehicle, tyre pressure, shock absorber, EUSAMA coefficient, Digital Image Correlation, diagnostics

1. Introduction

During operation, vehicles are subjected to several types of external loading that lead to forces and moments in their components. They are also under continuous kinematic and dynamic excitations with a wide frequency spectrum [1, 2]. Therefore, a vehicle should be considered as a complex vibrating system with many degrees of freedom. The vibrations are related to road surface irregularities, road infrastructure elements, acceleration and braking. They should be damped by the vehicle's suspension system [3–6]. However, some of these vibrations are transferred to the vehicle body. In addition, the body is also affected by vibrations resulting from the operation of the engine and drive system [2]. The main element that dampens vibrations in the vehicle and reduces their level is a shock absorber. Appropriate vibration damping is important because in the opposite case, it can lead to discomfort to passengers and be harmful to their health [7, 8). Over the years,

(*) Corresponding author.
E-mail addresses: J. Gonera (ORCID: 0000-0001-7758-2684) jaroslaw.gonera@uwm.edu.pl, T. Szymczak (ORCID: 0000-0003-2533-7200) tadeusz.szymczak@its.waw.pl,

efforts have been made to ensure a higher damping coefficient of shock absorbers by providing greater and better isolation of the driver and passengers from road conditions [8–10]. One way to improve comfort and better isolation from road conditions is to reduce the frequency and amplitude of vibrations as a result of the appropriate design and characteristics of shock absorbers [10–12]. The safety of passengers also depends on the design and technical condition of the suspension system elements [13]. Furthermore, it is worth emphasising that the parameters of the suspension system may be reduced during vehicle use, which may lower vehicle safety. It can be done by changes in values of vehicle weight and load distribution [14, 15]. Shock absorbers with a high vibration damping coefficient contribute to rapid damping of vibrations and, as a result, to improved driving stability [11].

In addition to the influence of the technical condition and design parameters of shock absorbers on vehicle handling when driving on uneven surfaces, they also affect cornering, as well as the acceleration and braking of vehicles [16]. This is related to the phenomenon of changing the mass distribution on individual vehicle wheels. In turn, as a result of changing the mass distribution on individual wheels, the damping coefficient of shock absorbers changes. Therefore, during the use of vehicles, there are continuous changes in the damping coefficient of shock absorbers. The values of this coefficient also depend on the values of the tyre pressure and its changes [17]. Tyre stiffness is closely correlated with the values of the tyre pressure and affects the values of the shock absorber damping coefficient [18]. As a result of differences in the stiffness and elasticity of the suspension system elements, the driving properties and stability of the vehicle may change [19]. In addition to the vehicle load and tyre pressure, the type of tyres and the ambient temperature may also affect the parameters of shock absorbers. In paper [20–22], it was shown that the ambient temperature and the temperature of the shock absorber have a significant impact on the values of the damping coefficient of shock absorbers. During the vehicle operation, the technical condition of shock absorbers changes. Therefore, the initial operating parameters of shock absorbers do not ensure stable vehicle handling under variable loading conditions and they are dependent on environmental conditions [19, 23]. A high level of reliability and proper technical condition of all components contribute to an increase in vehicle and road safety levels [24, 25]. In this case, one of the main parameters determining the level of safety is the technical condition and operating parameters of shock absorbers. When verifying the technical condition of shock absorbers, setting the nominal value of the tyre pressure is very important in terms of measurement results. The results of the paper [26] enabled to identify that tyre pressure has a significant influence on the diagnosis of the suspension system, it can highlight faults affecting the rolling resistance, but it does not have a main role in the maximum braking force value and the results of the diagnosis of the braking system on the roller stand.

The tyre pressure value, apart from its influence on the damping coefficient of shock absorbers, also affects many vehicle operating parameters such as braking distance for example. Both too-low and too-high tyre pressure values relative to the nominal pressure value extend the braking distance of vehicles [27]. Additionally, the braking distance is affected by the tyre tread height [28]. The tyre pressure also follows vehicle handling and passenger comfort. Pressure changes relative to the nominal values contribute to the generation of vibrations and vertical accelerations of the suspension system [29]. Reducing the tyre pressure below the nominal value lowers the stiffness of the tyres and suspension system. It also contributes to increased understeering of vehicles when driving on a curved track and reduced normal wheel loads. This significantly worsens vehicle control and reduces the level of safety [30]. Vehicles with too low tyre pressure tend to lose traction and are more prone to deviating from the driving line when driving on bends than those with tyre pressure in line with the nominal values [31]. In papers [32, 33], it was shown that increasing tyre pressure above the nominal value reduces the durability of the bituminous surface layer, and contributes to surface damage and rut formation. With decreasing tyre pressure, the noise level decreases. However, in addition to tyre pressure, the noise level is also influenced by tyre size and tyre compound composition [34]. The authors [35] showed that increasing driving speed contributes to the deterioration of vehicle stability and causes increased radial run-out of tyres and increased lateral tyre roll. Reducing the value of these parameters and improving vehicle stability can be achieved by increasing the tyre pressure [35]. Tyre pressure also has a significant impact on the fuel consumption value. This applies to both passenger cars and trucks. The tyre pressure higher value reduces fuel consumption [36]. This is related to the fact that at lower tyre pressure values, greater tyre deformation occurs, and therefore rolling resistance increases [37]. However, it should be emphasised that the changes in tyre pressure on the value of rolling resistance are strictly dependent on the type of tyre because tyres with low rolling resistance are less susceptible to changes in tyre pressure [38]. In turn, Ejsmont et al. [39] showed that there is an additional strong effect of tyre temperature, ambient temperature and road surface temperature on the value of rolling resistance. Moreover, it was found that the effect of tyre pressure on the rolling resistance force depends on the speed of the vehicles. At high speeds, the effect of pressure on rolling resistance is smaller because the tyres deform less due to a high value of centrifugal force [40].

During operation, a lowering in wheel pressure values can occur due to a flat tyre or the leakage of the connection between the tyre and the rim. It directly reduces road safety because the tyre tread does not have full contact with the road surface and the vehicle becomes unstable at driving and braking. Moreover, for safety reasons, vehicle users should care about wheel pressure values that align with the manufacturer's recommendations because this affects the comfort of travel and limits vehicle nominal driving parameters at a high-speed value. It is worth noting that wheel pressure changes can reduce the parameters of the suspension system and contribute to fuel consumption and exhaust emissions. For this, differences in wheel rotational speed can also be observed influencing a driving speed value. This limits the functioning of the ABS, ESP, etc. systems.

As it can be noticed, there are several similar papers in which the Authors analyse the influence of tyre pressure on the value of the shock absorber damping coefficient. However, they do not cover these changes depending on different tyre sizes. Moreover, the effect of tyre size on changes in pressure value significantly influences the shock absorber damping coefficient is also not considered. Therefore, this approach follows the problem. Moreover, efforts at using the DIC method to identify the size of tyre reaction and the value of the displacement of measurement points placed on the tyre, rim and body elements during changes in tyre pressure values are not presented.

For these reasons, two main stages are proposed. The first one considers the influence of tyre pressure values on the shock absorber damping coefficient of passenger cars at two different tyre sizes. The second stage captures tyre displacement/deflection and the movement of rim and body elements versus tyre pressure values at the digital image correlation (DIC) approach by PONTOS 5M.

2. Tested objects and experimental procedure

For the experiment, operated and non-operated SUVs (Sport Utility Vehicle) were employed (Tab. 1). This vehicle type was selected because it is the most popular category of passenger cars purchased in Europe. The changes in the shock absorber damping coefficient were analysed based on the differences in wheel pressure of twenty SUVs. These included vehicles equipped with tires of size 235/55 R19 (10 vehicles) and 235/65 R17 (10 vehicles). The tire sizes differed in the height of the cross-section, which was 129.25 mm and 152.75 mm, respectively.

Tab. 1. Details of SUV vehicles.

SUVs' technical features		
	A	B
Operated period	below 2 months	½ month
Mileage	1,000 km	50 km
Dimensions	4.6 × 1.9 × 1.6 [m]	4.6 × 1.85 × 1.68 [m]
Wheelbase	2.8 m	
Suspension type	Independent front axle suspension and independent multi-link rear axle suspension as well as rack and pinion steering	Independent front axle suspension in the form of a McPherson strut, while the rear axle was equipped with an independent, multi-link suspension
Engine type and its volume	Spark-ignition engines with a capacity of about 2.0 dm^3	Spark-ignition internal combustion engine with a capacity of about 1.5 dm^3
The curb weight	1,700 kg	1,650 kg

SUVs' technical features		
	A	B
Permissible load capacity	500 kg	450 kg
Tyres' size	235/65 R17 and 235/55 R19	235/55 R19

Concerning the limited region for the test, i.e. vehicle inspection station, the experimental procedure does not follow the influence of road conditions, vehicle load, and tyre composition. It was divided into three stages covering the vehicles indicated in Tab. 1. This was conducted for the following changes in the shock absorber damping coefficient values at different tyre pressure values.

The first approach used the Beissbarth STL7000 diagnostic line (Fig. 1a) to measure the shock absorber damping coefficient (EUSAMA coefficient). It was equipped with the Micro-Swing 6200 module for testing the suspension system of passenger cars. In addition, to measuring the coefficient value, the diagnostic line also enables the braking efficiency coefficient and the half-alignment of the wheels to be estimated. The tests were conducted at the tyre pressure value changes for 0.02 MPa.

During the second approach, the Unimetal 5000 diagnostic line was used for measuring the EUSAMA coefficient (Fig. 1b) under the same conditions as the Beissbarth STL7000 diagnostic line was employed.

The frequency of vibration excitation in stations using the EUSAMA method reaches 25 Hz, and the displacement amplitude of the measuring plates on which the vehicle stands was equal to 6 mm. It is worth emphasising that diagnostic lines based on the EUSAMA method are the only devices approved for checking the technical state of shock absorbers. This coefficient is determined from the following relationship:

$$W_{EUSAMA} = \frac{P_{d\,min}}{P_s} \cdot 100\ [\%], \text{ where:} \quad (1)$$

$P_{d\,min}$ – minimum dynamic pressure on the measuring plate during the test;

P_s – static pressure on the measuring plate during the test.

Both diagnostic lines were used because the experimental procedure stages were covered in two different scientific research units i.e. University of Warmia and Mazury (Olsztyn, Poland) and Motor Transport Institute (Warsaw, Poland).

The 3D movements of measurement points cemented on the tyre, rim, and body elements concerning changes in tyre pressure were followed using the digital image correlation (DIC) method, Fig. 2. It was delivered in the PONTOS 5M – GOM device. The system enabled capturing displacement of components' values in the 3D coordinate system, creating files, courses, photos, and movies. Additionally, DIC results have supported the analysis of differences in the shock absorber's damping coefficient as a function of tyre pressure value.

(a)

(b)

Fig. 1. A view of the vehicle diagnostic line to measure the EUSAMA coefficient: (a) Beissbarth STL7000, (b) Unimetal 5000.

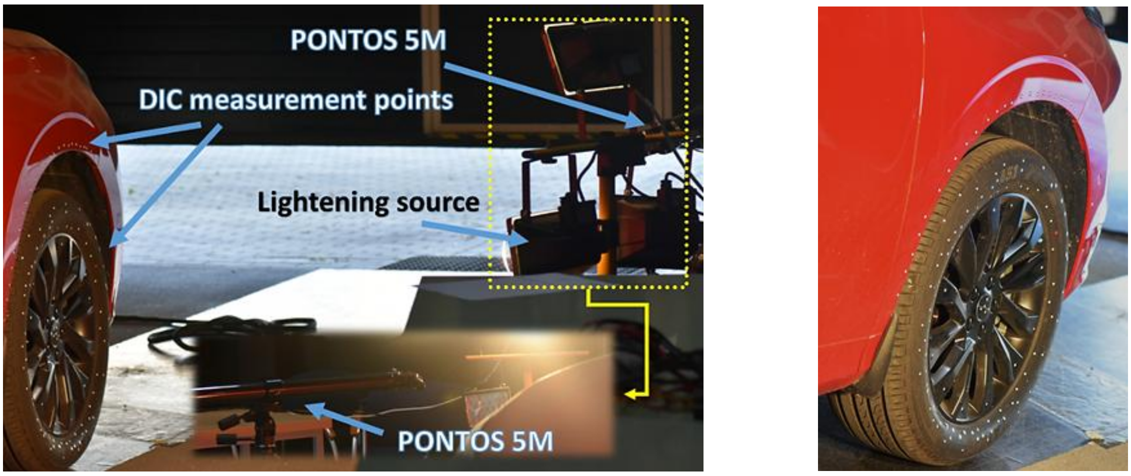

(a) (b)

Fig. 2. Details of the experiment on an SUV and PONTOS 5M: (a) components, (b) measurement points' distribution.

The same tyre pressure value changes were used in all the examined cars at all three stages, Table 2. Measurements began with a tyre pressure of 0.30 MPa, next, the tyre pressure was reduced at its step value of 0.02 MPa up to 0.10 MPa, finally. This tyre pressure change was used for both the front and rear axles of the vehicles. The nominal tyre pressure value for the front and rear axles of the cars was equal to 0.24 MPa Table 2.

Tab. 2. Details of tire pressure value.

	Tire pressure value [MPa]										
Front axle	0.30	0.28	0.26	0.24	0.22	0.20	0.18	0.16	0.14	0.12	0.10
Rear axle	0.30	0.28	0.26	0.24	0.22	0.20	0.18	0.16	0.14	0.12	0.10

For the work, three types of vehicle speeds were defined.

- The actual linear speed is the speed that results from the rolling circumference of the wheel at the actual wheel pressure.
- Calculated linear speed is the speed calculated from equation (1), taking into account the dynamic radius of the wheel.
- The speed indicated on the odometer and recorded by the vehicle's controls is the speed resulting from the rolling circumference of the wheel at nominal wheel pressure (0.24 MPa).

3. Results for the EUSAMA coefficient

3.1. Shock absorber damping coefficient in values

The results for changes in the shock absorber damping coefficient values were analysed depending on the differences in wheel pressure of twenty SUVs, Fig. 3-Fig. 4. Fig. 3 and Fig. 4 presents the changes in the parameter as a function of the pressure values of the wheels for a tyre size 235/55 R19 (blue) and 235/65 R17 (red).

In the case of tyres with a higher profile of 65% (Fig. 3a), a linear relationship for the shock absorber damping coefficient can be seen at all pressure values used. At the lowest pressure value, i.e. 0.10 MPa, the average value of the damping coefficient was equal to 90%. The value of this coefficient decreased proportionally, up to a value of 62%. This was because the lower pressure made the tyre softer, and the damping coefficient of the shock absorbers had a higher value.

For tyres with a lower profile (55%), the changes in values of the damping coefficient were not linear. This relationship can be divided into two regions. In the first one, a linear relationship can be observed at reducing the wheel pressure from 0.30 MPa to 0.16 MPa. With a decrease in the pressure, the average value of the damping coefficient of the shock absorbers increased proportionally. Then, from this value of the pressure, reducing it in subsequent stages, the value of the damping coefficient of the shock absorbers decreased. This was because a low-profile tyre is significantly stiffener at its low-pressure value, and it does not absorb vibration, and additionally, it stiffens the suspension system. Based on the data presented in Fig. 3, it can be noticed that the size of the tyre, and in particular its profile, has a significant influence on the relationship between changes in the coefficient of damping effectiveness of shock absorbers and wheel pressure.

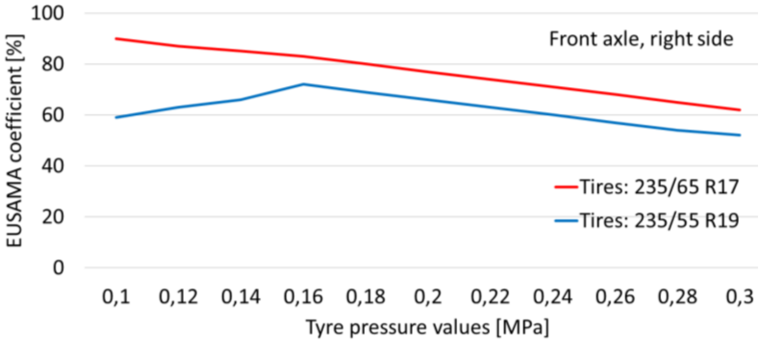

(a)

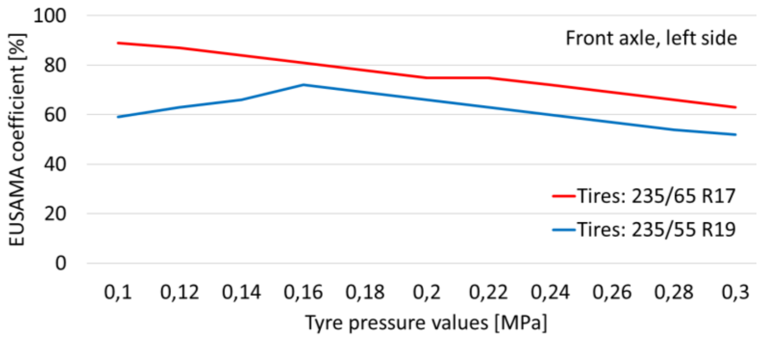

(b)

Fig. 3. The EUSAMA coefficient versus the tyre pressure values for: (a) the right-side and (b) left-side front axles at two tyres' different sizes

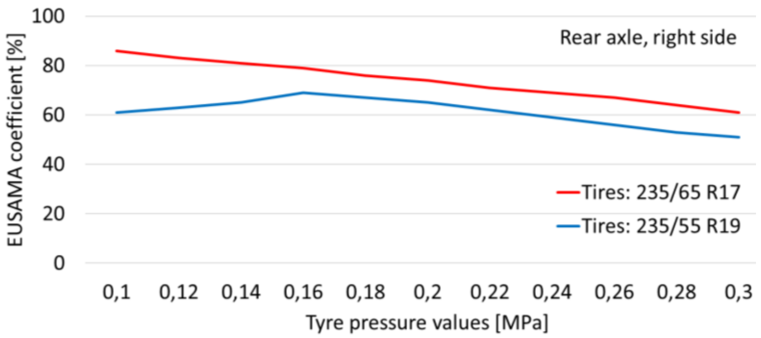

(a)

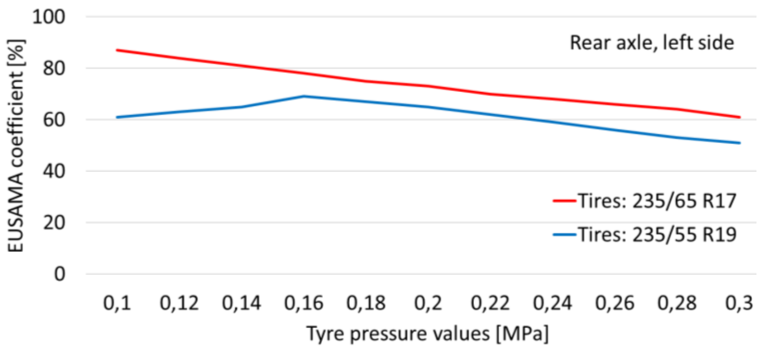

(b)

Fig. 4. The EUSAMA coefficient versus the tyre pressure values for; (a) the right-side rear and (b) the left-side rear axles at two tyres' different sizes

Similar changes in the shock absorber damping coefficient as a function of tyre pressure values of the front left wheel, Fig. 3b but for this case a 235/65 R17 tyre response was not linear for the pressure range value used. The slight differences in the changes in the coefficient depending on the pressure values in the wheels for both front wheels result from the uneven distribution of mass on the vehicle's front axle, between their right and left sides.

3.2. Shock absorber damping coefficient in statistic assessment

It was also determined, that the shock absorber damping coefficient depends on the tyre size, Fig. 5, Fig. 6. In the case of the left front wheel, Fig. 5b, significant differences between the coefficient values depending on the tyre size at the same pressure values were presented. They were also observed at the 235/55 R19 wheels, while for the 235/65 R17 ones, changes occurred for the pressure from 0.20 MPa to 0.22 MPa.

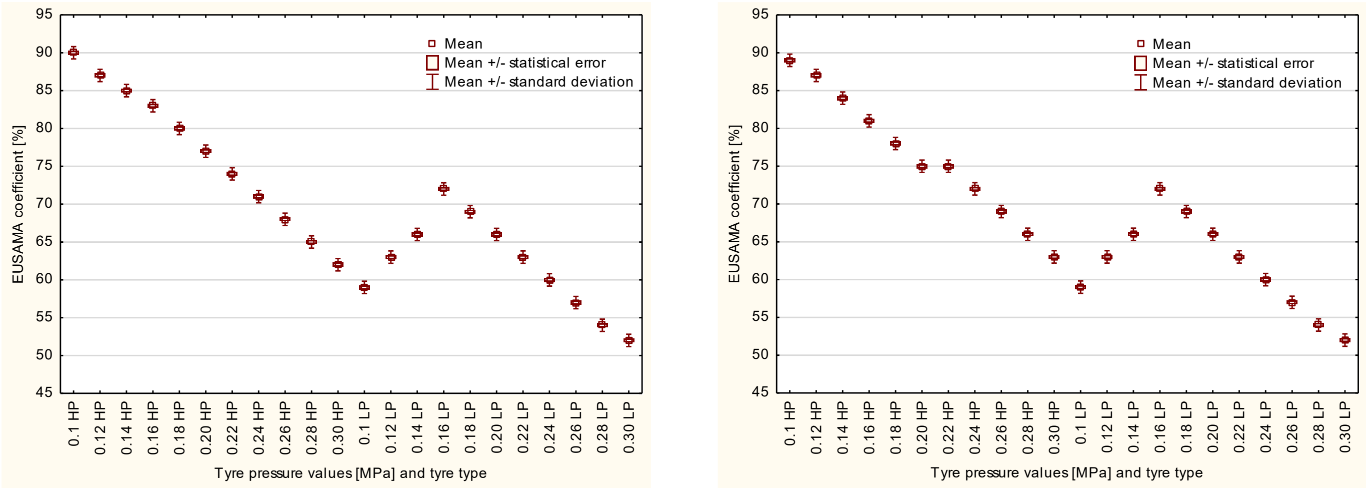

(a) (b)

Fig. 5. The EUSAMA coefficient versus the tyre pressure values and tyre type for: (a) right-side front axle, (b) (left-side front axle, where: HP - high profile tyre (235/65 R17), LP - low profile tyre (235/55 R19).

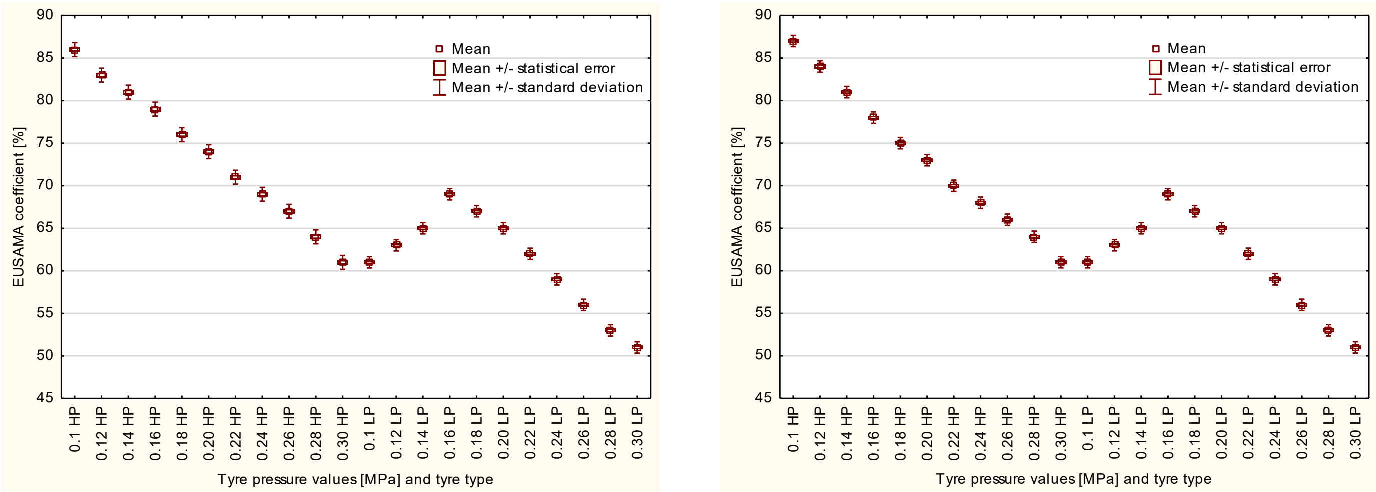

(a) (b)

Fig. 6. The EUSAMA coefficient versus the tyre pressure values and tyre type for: (a) right-side rear and (b) left-side rear axles, where: HP - high profile tyre (235/65 R17), LP - low profile tyre (235/55 R19).

This problem is also presented in Fig. 6, which reflects the statistical assessment for the rear right and rear left wheels. In the case of the higher and lower profile tyres, important changes were found between the values of the damping coefficient of the shock absorbers and the tyre pressure. Changes were also found between the shock absorber damping coefficient values and the tyre type.

Comparing (Fig. 7) results and the previous ones, it can be seen that in this case, there is a clear change in the damping coefficient at a tyre pressure of 0.16 MPa.

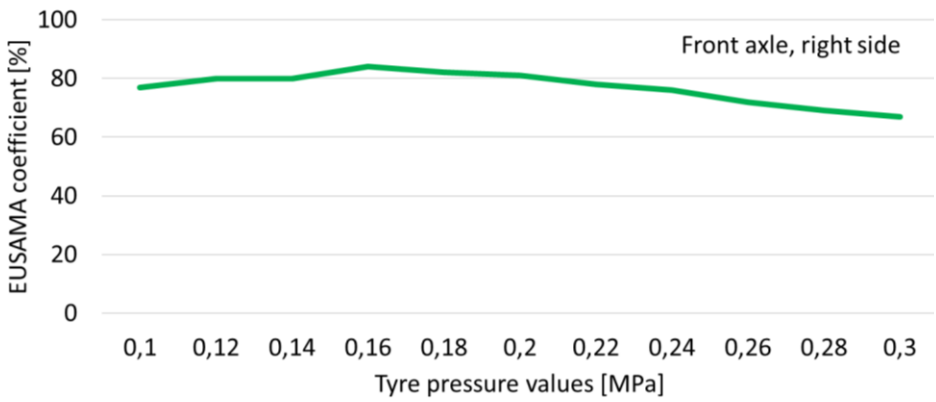

Fig. 7. EUSAMA coefficient trend versus the tyre pressure right-side front axle for the not-operated SUV.

4. DIC results for the deflection of a tyre for different values of its pressure

Figure 8a shows the results of digital image correlation (DIC) measurements at a tyre pressure of 0.28 MPa. This was collected after reducing the pressure by 0.02 MPa. In the next steps, the pressure values were also reduced by 0.02 MPa. In those cases, measurement markers were cemented on the front right fender and bumper of the car and the tyre rim for covering examined region behaviour in the 3D coordinate system. Most of them have followed tyre reactions because this vehicle component is crucial in road safety. The X-axis displacement has reflected a vehicle's main axis while the other ones, i.e. Y- and Z-axes, have captured perpendicular directions for covering its height and width.

After reducing the pressure from 0.30 MPa to 0.28 MPa (Fig. 8a), very small changes in the displacement of points in the X-axis direction were observed. The displacement values in the Z-axis direction were almost two times higher. In the case of the tyre, most of the inspected sections located in its upper part (above the wheel hub) moved outside the vehicle, and other ones located in its lower part (below the wheel hub) moved inside the vehicle. In the Y-axis direction, i.e. in the vertical axis, much larger displacements of points were found. Even with a pressure reduction of 0.02 MPa, displacement values exceeding 0.81 mm were found. All points moved towards the road. The highest displacement values occurred in the upper part of the tyre, while smaller ones were found in the lower part of the tyre. It was related to the relatively high stiffness of this 235/55 R19 tyre region.

Figure 8b shows the displacement differences during the wheel pressure value change up to 0.22 MPa. In comparison to the previous data, significant increases in the displacement values of the analysed regions were manifested in all directions. In the case of the tyre, it can be observed that some of the measurement points moved towards the front of the vehicle and some towards the rear - this is related to the loss of tyre stiffness. Similarly, the loss of tyre stiffness is evidenced by the displacement in the direction of the Z-axis. Most of the points in the upper part of the tyre moved towards the Z-axis outside the tyre. On the other hand, most of the points in the lower part of the tyre moved towards the interior of the vehicle.

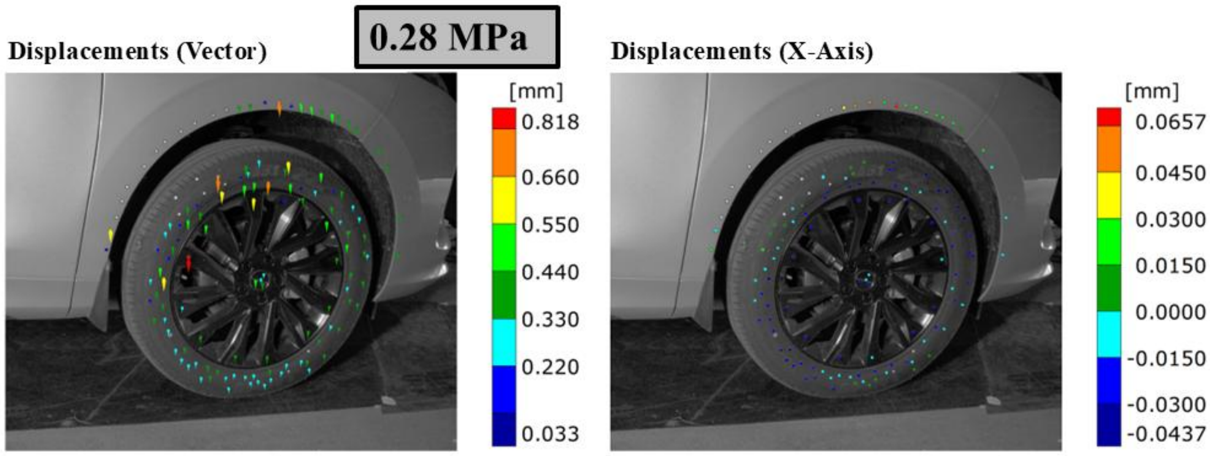

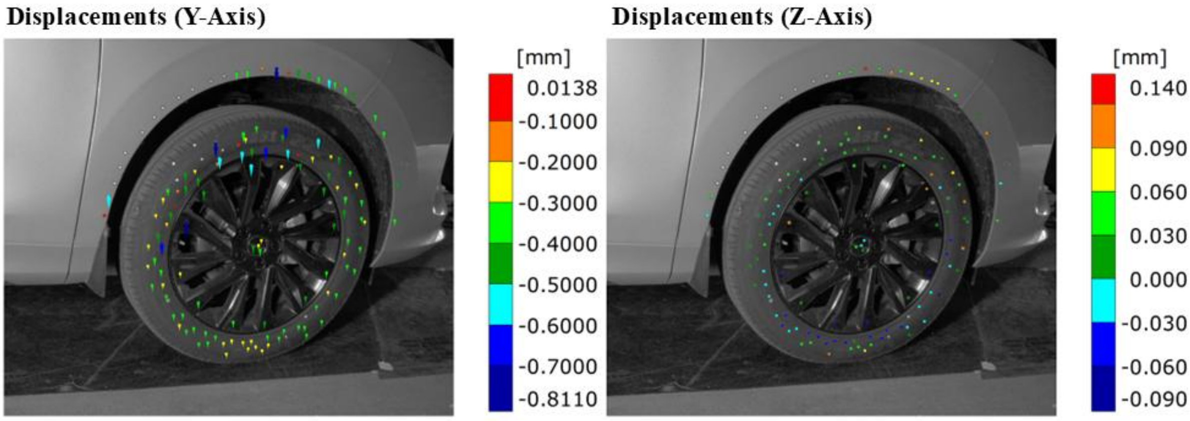

(a)

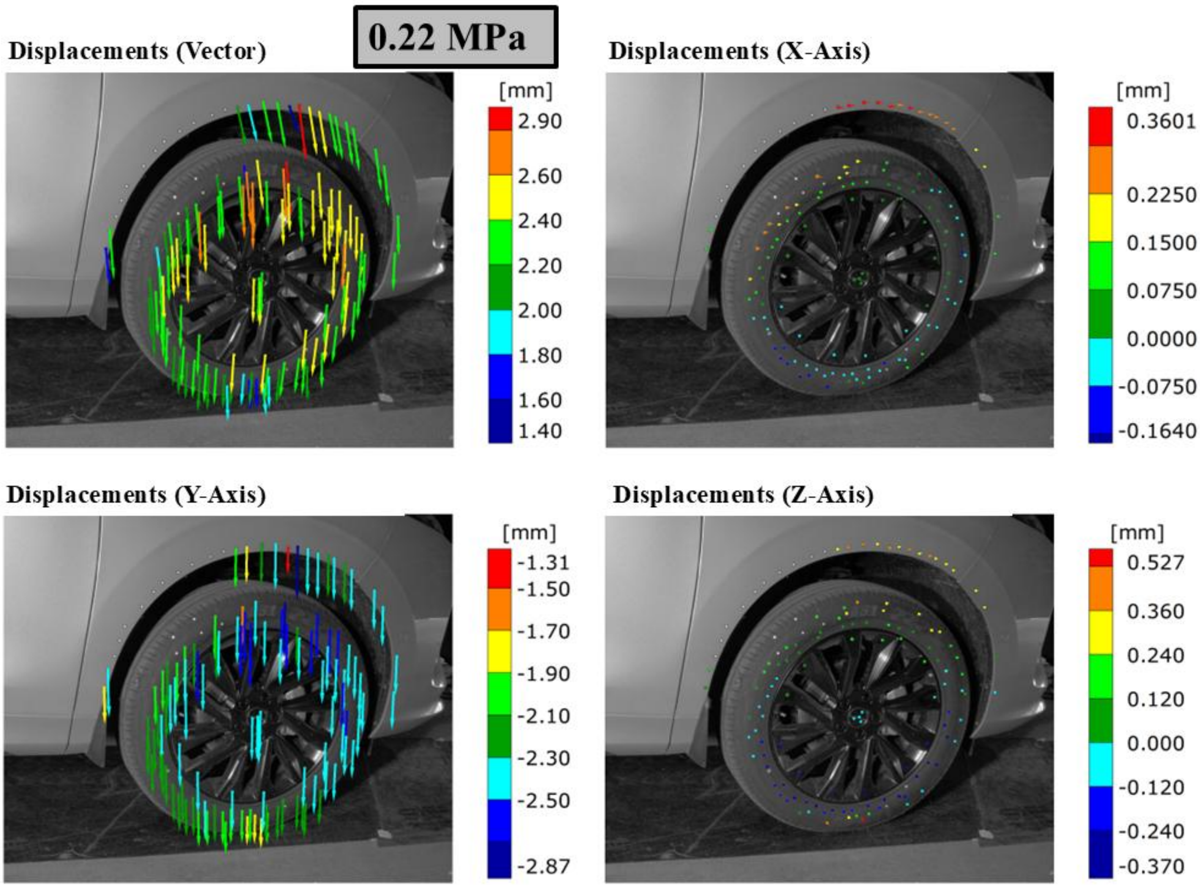

(b)

Fig. 8. Displacement components and their resultant vector in the 3D coordinate system at a tire pressure value of 0.28 MPa (a) and 0.22 MPa (b)

In the Y-axis direction, the highest displacements were found. The largest range of changes occurred in the upper part of the tyre, above the wheel hub and on the fender. Moreover, in the case of the tyre, not only differences in the displacement of points were found between the upper and lower parts of the tyre, which were influenced by the tyre stiffness. Clear differences in the displacement of points also occurred between the front and rear parts of the tyre with the wheel rotation axis. Higher displacement values occurred in the front part of the tyre. This was related to the change in the mass distribution during the reduction of the pressure in the wheels and, as a result, the reduction in the vehicle's ground clearance on the front right side of the bodywork.

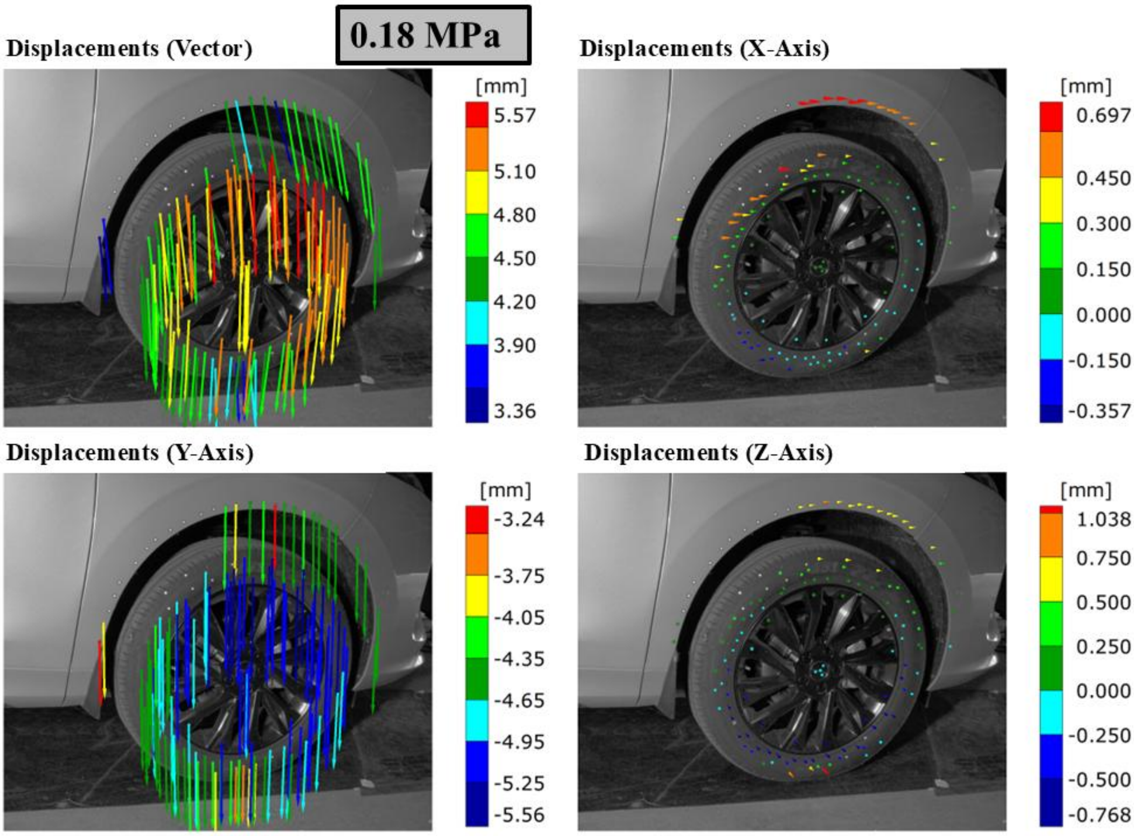

(a)

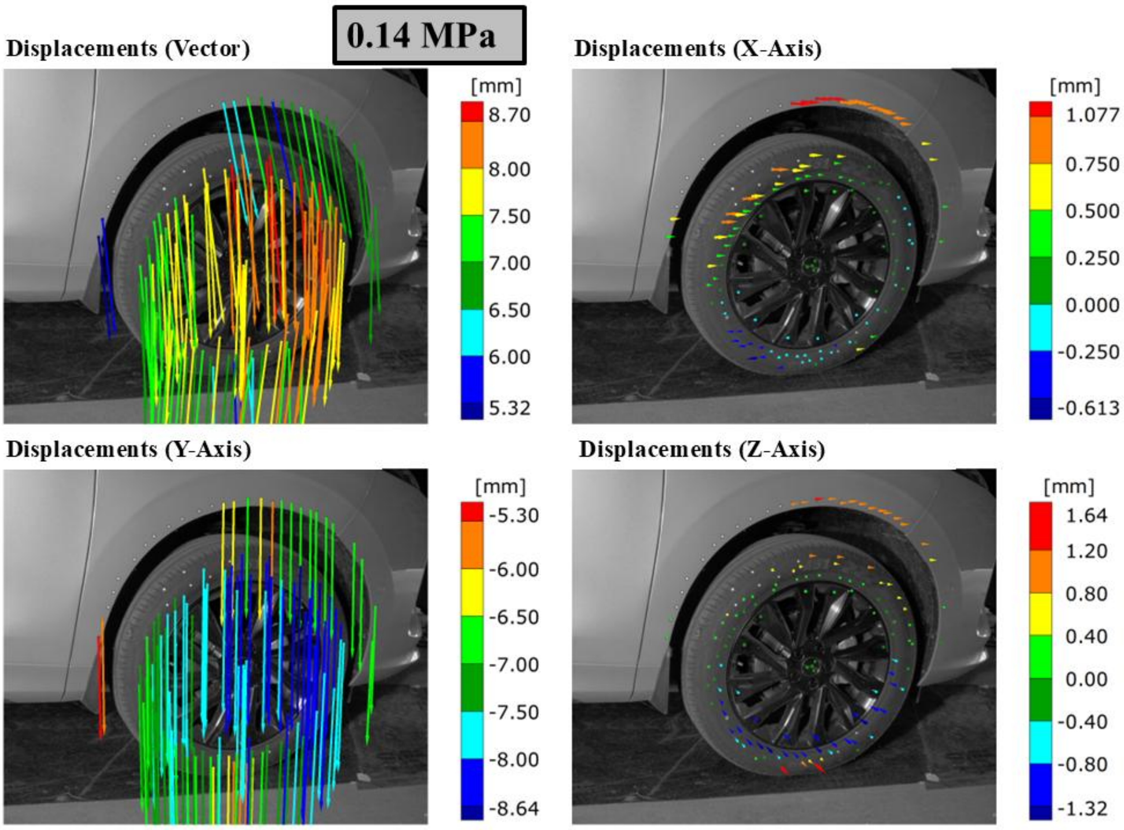

(b)

Fig. 9. Displacement components and their resultant vector in the 3D coordinate system at a tyre pressure value of 0.18 MPa (a) and 0.14 (b)

The DIC results captured at a tyre pressure of 0.18 MPa are presented in Fig. 9a. Comparing them with the results at a tyre pressure of 0.22 MPa (Fig. 8b), it can be concluded that the changes in the position of the analysed points were the same. In all axes (X, Y and Z), the displacements of individual points occurred in the same direction as before, however, the displacement values were higher. It is possible to distinguish regions on the tyre with smaller and larger displacement values , which are the result of the influence of changes in tyre stiffness and differences in mass distribution as a result of reducing the body clearance, together with lowering the pressure in the wheel.

Figure 9b compares the positions of the measurement regions on the tyre, fender, rim and bumper for a wheel pressure of 0.14 MPa. Analysing the displacements at a wheel pressure of 0.14 MPa, it can be noticed that in comparison with the previous results, the displacement feature has not changed in this case either. There are significant increases in the displacement value of measurement individual points resulting from an even greater reduction in wheel pressure. In the Z-axis direction, the points moved by a maximum of 1.64 mm. The points located on the mudguard moved outwards. Similarly, most of the points located in the upper part of the tyre, above the wheel hub, moved outwards. On the other hand, many points in the lower part of the tyre moved inwards.

There was a clear collapse of the lower part of the tyre, which was stiffer in this area. In the lower part, the points located at the inner part of the tyre, near the tyre bead, i.e. the connection with the rim, moved by the greatest amount towards the inside of the vehicle. This lower part feature results from the loss of its stiffness and increases the risk of the tyre bead detaching from the rim and the tyre falling off the rim. This may threaten the vehicle's safety and create the risk of an accident. Also, at a pressure in the wheels of 0.14 MPa, the displacement greatest values in the direction of the Y-axis were found. Also at this pressure value, there were clear differences between the displacement values of the analysed points located in the lower and upper part of the tyre, as well as between the position of the points in the front and rear part of the tyre concerning the axis of rotation of the wheel. This is the result of the change in mass distribution when reducing the vehicle's ground clearance and results in an uneven distribution of the tyre load.

The deflection of the tyre at the DIC approach was visible at all tyre pressure values, Fig. 8-Fig. 9. This was expressed by very small (Fig. 8) and very high (Fig. 9) values indicating changes in the tyre response due to the pressure differences. It shows that besides the Y-axis dominant deflection, the component reacts in a vehicle's main longitudinal and perpendicular axes, Fig. 9. From the operating stage of view the X-deflection creates additional resistance for driving while the Z-deflection limits holding the vehicle in corners.

Changes in the component displacement values at individual pressure differences for the front right wheel follow their courses (Fig. 10a). The results show that the X and X displacement courses are very similar, while the Y ones is completely different. As was presented earlier, the deflection in the Y-axis direction plays a dominant role in the tyre behaviour, creating the resultant displacement vector values, Fig. 10.

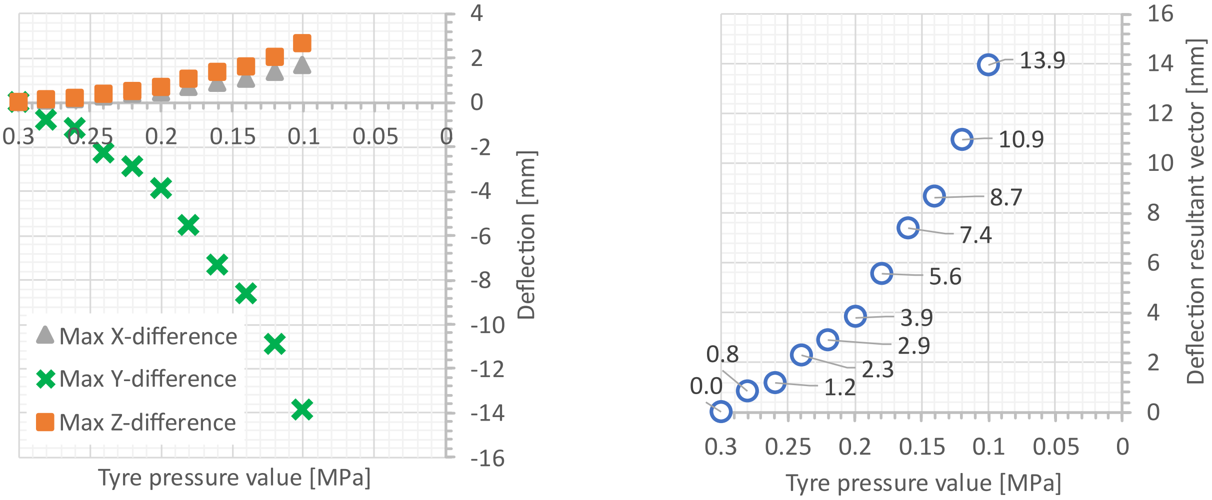

(a) (b)

Fig. 10. Changes in values of displacement components (a) and resultant vector (b) versus tyre pressure value at the DIC approach

In the more complex analysis, the following sentence can be formulated: the relatively large values between the minimum and maximum positions of points in the X and Z axis direction resulted from the fact that some of the points in the direction of these axes tended to have negative values while some to positive ones. In the case of the Y axis, however, all points moved towards negative values. Therefore, the displacement values in the X and Z-axis directions are smaller than in the Y-axis.

The tyre displacement points in the direction of the X and Z axes mainly contribute to the increase of the tyre's contact surface with the ground. This directly translates into an increase in the vehicle's resistance to motion, i.e. indirectly into an increase in fuel consumption and an increase in exhaust emissions [41, 42]. To reduce fuel consumption, it is necessary to monitor the states of tire-road interaction as well as the rolling resistance during vehicle performance [41]. Rolling resistance is the major cause of the energy loss in pneumatic tires and thus, its reduction leads to substantial energy savings, CO_2 emission reductions, and more mileage [42]. It may also affect the vehicle's handling, while the Y displacement causes a decrease in the height of the tyre profile, and therefore the dynamic radius of the wheel. This directly translates into a change in the indicated on the odometer and recorded by the vehicle's controls driving speed, and may affect the operation of driving assistance systems and those that increase the level of active safety of vehicles.

Based on the results, it was possible to determine the changes in the vehicles' linear speed value as a function of tyre pressure differences. For this purpose, it was necessary to use relationship No. 1. As a result of the change in the dynamic radius of the wheel associated with a tyre height, differences in the linear speed of the vehicle occurred.

$$V = \frac{2 \cdot \pi \cdot n_m}{60 \cdot i_{ds}} \cdot r_w \text{ , where} \tag{2}$$

V – vehicle linear speed;

n_m – rotation engine speed;

i_{ds} – drivetrain ratio;

r_w – dynamic wheel radius.

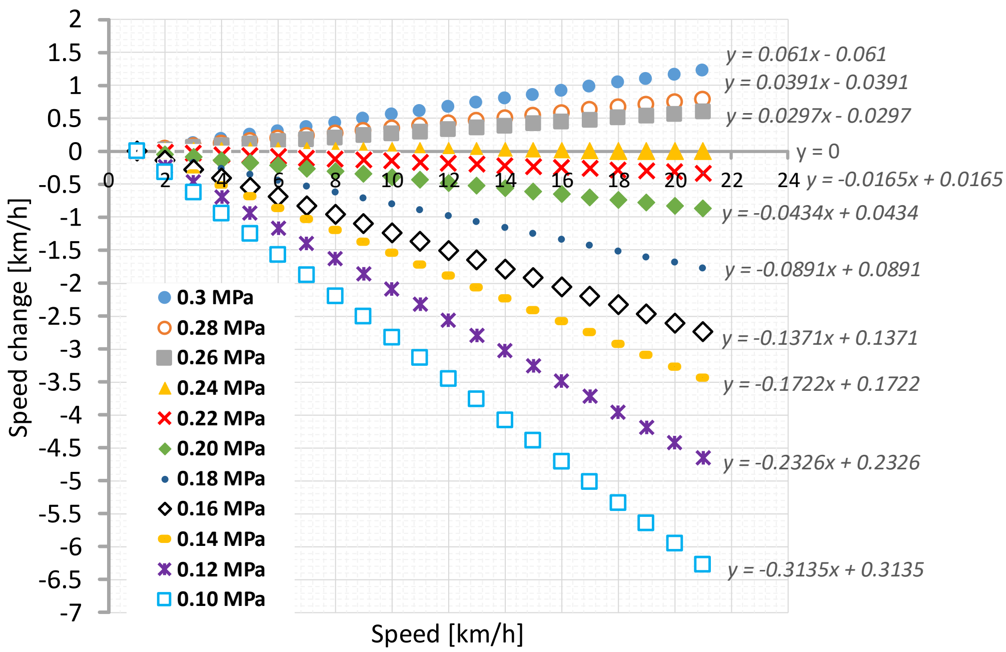

Fig. 11. The SUV speed versus tyre pressure

Fig. illustrates the changes in the vehicle's linear speed value at different tyre pressures. For each tyre pressure value, a linear relationship was observed between the change in speed and the actual linear vehicle speed. For the tested vehicle, the nominal tyre pressure set by the manufacturer on the front axle is 0.24 MPa. At this tyre pressure value, the speed indications and its recorded value are consistent with the vehicle manufacturer's assumptions. Because of the above, it was assumed during the calculations that at a pressure of 0.24 MPa, the dynamic radius value is the nominal value. Therefore, a linear relationship can be observed. On the other hand, an increase in tyre pressure (0.26, 0.28 and 0.30 MPa) above the nominal value contributed to an increase in the dynamic radius of the wheel. In this case, changes in linear speed can be noticed.

Relatively small values of the increase in the actual linear speed of the vehicle are visible. At a speed of 200 km/h, these changes reach about 1.2 km/h. In the case of reducing the tyre pressure value below its nominal one, driving speed values decreased. At a speed of 200 km/h, these changes reach about 1.8 km/h at a tyre pressure of 0.18 MPa. In the case of the remaining tyre pressure values analysed during the tests, there were even greater differences between the indicated and recorded linear speed and the actual linear speed. At a tyre pressure of 0.10 MPa, the speed change was about 6.3 km/h. A drop in tyre pressure below the nominal value significantly reduced the indicated and recorded vehicle speed. This causes differences between the actual linear vehicle speed and the speed indicated to the user, and may also affect the operation of driving assistance systems, which are elements of active vehicle safety.

5. Conclusion

The performed experiment and its results can be instrumental because they follow the practical aspect of vehicle diagnostics employing a new approach at DIC method to the problem considered. It is related to:

(a) the identification of the influence of wheel pressure changes on the values of the passenger car shock absorbers' damping coefficient, depending on the size of the tyres,

(b) the behaviour of the vehicle component using the digital image correlation (DIC) method at different tyre pressure values.

It can be concluded that there is a relationship between the values of the shock absorber coefficient and wheel pressure. These changes were dependent on the tyre size. The DIC method at the PONTOS 5M system can be used to cover the behaviour of tyre types. Thanks to this, it is possible to identify the influence of tyre pressure value on tyre deformation in three planes and the vehicle's operating parameters. It is possible to indicate the regions of the tyre with the greatest deformation level. It was found that with decreasing pressure in the wheels, the analysed sections moved in all three coordinates. At each pressure value, there were clear differences for the displacement regions located in the lower and upper sections of the tire, as well as between the front and rear ones, relative to the axis of rotation of the wheel.

The approach has enabled to capture the damping coefficient values of passenger car shock absorbers and changes in tire deflection as well as differences in driving speed. In the case of vehicles with softer tyres (with a higher profile) of size 235/65 R17, the value of the damping coefficient of shock absorbers decreased linearly with increasing tyre pressure. The low-profile tyre (235/55 R19) is harder, and at low tyre pressure, it does not absorb vibration damping and additionally stiffens the suspension system.

The largest response at DIC measurements was found in the Y-axis direction, i.e. the vertical deflection, to the road. The largest reaction of the component was observed on the fender as well as in the upper part of the tyre, above the wheel hub, and in the front part of the tyre. In the case of the tyre, it can be observed that the X-axis displacement component moved towards the front of the vehicle, and some towards the rear as a result of the tyre stiffness reduction. From the operational point of view, the deflection of the X-axis creates additional resistance while driving, while the deflection of the Z-axis limits the vehicle's grip on bends.

For each tyre pressure value, a linear relationship was observed between the change in speed and the actual linear vehicle speed. At a pressure of 0.24 MPa, the dynamic radius reached the nominal value. An increase in tyre pressure above the nominal value contributed to an increase in the dynamic radius of the wheel, therefore, changes in linear speed can be observed. Relatively small increases in the actual linear speed of the vehicle were visible. In the case of reducing the tyre pressure below the nominal value, the indicated on the odometer and recorded by the vehicle's controls driving speed decreased. The DIC results indicate that the tyre behaviour at its different pressure values was not homogeneous because Y-deflection values for points symmetrically arranged concerning it did not reach the same values. For this case, it sounds the tyre construction may be improved. During the operation of vehicles, it is important to maintain proper wheel pressure, because it enables reaching the required level of road traffic safety. Tyre pressure should be checked frequently in older cars or monitored online in new ones.

Reference

1. Xu G, He W, Chen F, Shen H, Li X. Automatic and Accurate Vision-Based Measurement of Camber and Toe-In Alignment of Vehicle Wheel. IEEE Transactions on Instrumentation and Measurement 2022; 71. DOI: https://doi.org/10.1109/TIM.2022.3216382.
2. Gonera J, Napiórkowski J. Analysis of the effect of passenger car design on floor panel wear. Measurement 2023; 220: 1-11. DOI: https://doi.org/10.1016/j.measurement.2023.113440.
3. Ahrens G, Dellmann T, Gies S, Hecht M, Hefazi H, Henke R, Pischinger S, Schaufele R, Tegel O. Applications in Mechanical Engineering. Transport Systems. Würzburg, Springer Science+Business Media: 2009. https://doi.org/10.1007/978-3-540-30738-9_13
4. Aguilar JJ, Sanz M, Guillomía D, Lope M, Bueno I. Analysis, characterization and accuracy improvement of optical coordinate measurement systems for car body assembly quality control. International Journal Advanced Manufacturing Technology 2006; 30: 1174-1190. DOI: https://doi.org/10.1007/s00170-005-0143-5.
5. Livesey WA, Robinson A. The repair of vehicle bodies. Oxford: Butterworth-Heinemann: 2006. https://doi.org/10.4324/9780080459813
6. Wallentowitz H. Virtuelle Fahrzeugentwicklung–Netzwerkeals Voraussetzungenzur Problemlosung; Erfolg in Netzwerken. Berlin, Springer – Verlag Berlin Heidelberg: 2002. https://doi.org/10.1007/978-3-642-56175-7_6
7. Ramalingam M, Jebaseelan D. The effect of vibration characteristics of an automotive seating system on ride comfort - A finite element study. ARCHIVE Proceedings of the Institution of Mechanical Engineers Part C Journal of Mechanical Engineering Science 2019; 223: 6588-6601. DOI: https://doi.org/10.1177/0954406219858172.
8. Shao X, Naghdy F, Du H, Qin Y. Coupling effect between road excitation and an in-wheel switched reluctance motor on vehicle ride comfort and active suspension control. Journal of Sound and Vibration 2018; 443: 683-702. DOI: https://doi.org/10.1016/j.jsv.2018.12.012.
9. Al-Zughaibi A, Xue Y, Grosvenor R. A new insight into modelling passive suspension real test rig system with consideration of nonlinear friction forces. Proceedings of the Institution of Mechanical Engineers Part D Journal of Automobile Engineering 2018; 1-26. DOI: https://doi.org/10.1177/0954407018764942.
10. Omar M, El-Kassaby MM, Abdelghaffar WA. Parametric numerical study of electrohydraulic active suspension performance against passive suspension. AEJ - Alexandria Engineering Journal 2018; 57: 3609-3614. DOI: https://doi.org/10.1016/j.aej.2018.05.007.
11. Bae S, Lee JM, Choi WJ, Yun JR, Tak TO. Axiomatic approach to the kinematic design of an automotive suspension system with the McPherson strut type. International Journal of Vehicle Design 2003; 31: 58-71. DOI: https://doi.org/10.1504/IJVD.2003.002047.
12. Durmaz BE, Kacmaz B, Mutlu I, Turan Söylemez M. Implementation and Comparison of LQR-MPC on Active Suspension System. In 10th International Conference on Electrical and Electronics Engineering (ELECO). Bursa, Turkey: 2017.
13. Hyniova K. One-Quarter-Car Active Suspension Model Verification. In The 2016 International Conference Applied Mathematics, Computational Science and Systems Engineering ITM Web of Conferences: 2017. https://doi.org/10.1051/itmconf/20170903003
14. Shim T, Velusamy PC. Suspension design and dynamic analysis of a lightweight vehicle. International Journal of Vehicle Design 2007; 43: 258-280. DOI: https://doi.org/10.1504/IJVD.2007.012307.
15. Vidya V, Dharmana MM. Model Reference Based Intelligent Control of an Active Suspension System for Vehicles. In International Conference on Circuit, Power and Computing Technologies (ICCPCT): 2017. https://doi.org/10.1109/ICCPCT.2017.8074362
16. Dukkipati RV, Vallurupalli SS. Smart active suspension to counteract dynamic load changes during critical manoeuvres. JSME International Journal Series C 2000; 43: 259-272. DOI: https://doi.org/10.1299/jsmec.43.259.
17. Gonera J. Influence of the size and distribution of load on the damping coefficient of shock absorbers in passenger vehicles. Advances in Science and Technology Research Journal 2020; 14 (4): 185-194 .DOI: https://doi.org/10.12913/22998624/127356.
18. Zuska, A, Jackowski J. Influence of Changes in Stiffness and Damping of Tyre Wheels on the Outcome of the Condition Assessment of Motor Vehicle Shock Absorbers. Energies 2023; 16: 3876. DOI: https://doi.org/10.3390/en16093876.
19. Shi Q, Peng C, Chen Y, He J. Robust kinematics design of MacPherson suspension based on a double-loop multi-objective particle swarm optimization algorithm. Proceedings of the Institution of Mechanical Engineers Part D Journal of Automobile Engineering 2019; 223: 3263-3278. DOI: https://doi.org/10.1177/0954407018821556.
20. Nikolay P. Influence of shock absorber temperature on vehicle ride comfort and road holding. MATEC Web Conferences 2017; 133: 02006. DOI: https://doi.org/10.1051/matecconf/201713302006.
21. Hryciów Z, Rybak P, Gieleta R. The influence of temperature on the damping characteristic of hydraulic shock absorbers. Eksploatacja i

Niezawodność - Maintenance and Reliability 2021; 23: 346–351. DOI: https://doi.org/10.17531/ein.2021.2.14.
22. Hryciów, Z. An Investigation of the Influence of Temperature and Technical Condition on the Hydraulic Shock Absorber Characteristics. Applied Sciences 2022; 12: 12765. DOI: https://doi.org/10.3390/app122412765.
23. Chen B, Liu Y, Shi W. Suspension Optimization Design and Virtual Prototype Simulation Analysis of FSAE Racing Car. Journal of Physics Conference Series 2019; 1176. DOI: https://doi.org/10.1088/1742-6596/1176/5/052084.
24. Gonera J, Napiórkowski J. Model for forecasting the geometry of the floor panel of a passenger car during its operation. Eksploatacja i Niezawodność - Maintenance and Reliability 2018; 20(4): 689-695. DOI: http://dx.doi.org/10.17531/ein.2018.4.20.
25. Rychlik A, Vrublevskyi O, Prokhorenko A. Modelling of the diagnostic station operation process to identify damage to the wheel rim structure. Journal of Mechanical Science and Technology 2019; 33 (9): 4129-4138. DOI: https://doi.org/10.1007/s12206-019-0808-x.
26. Toma M, Andreescua C, Stan C. Influence of tire inflation pressure on the results of diagnosing brakes and suspension. Procedia Manufacturing 2018; 22: 121-128. DOI: https://doi.org/10.1016/j.promfg.2018.03.019.
27. Stokłosa J, Bartnik M. Influence of tire pressure on the vehicle braking distance. 60The Archives of Automotive Engineering – Archiwum Motoryzacji 2022; 97(3). DOI: https://doi.org/10.14669/AM/155136.
28. Wang Y, Hu J, Wang F, Dong H, Yan Y, Ren Y, et al. Tire Road Friction Coefficient Estimation: Review and Research Perspectives. Chine Journal of Mechanical Engineering 2022; 35(1): 6. DOI: https://doi.org/10.1186/s10033-021-00675-z.
29. Hamed M, Tesfa B, Aliwan M, Li G, Gu F, Ball AD. The Influence of Vehicle Tyres Pressure on the Suspension System Response by Applying the Time-Frequency Approach. In Proceedings of the 19th International Conference on Automation & Computing. Brunel University, London, UK: 2013.
30. Parczewski K. Effect of tyre inflation pressure on the vehicle dynamics during braking manoeuvre. Eksploatacja i Niezawodnosc – Maintenance and Reliability 2013; 15(2): 134-139. DOI: https://doi.org/10.1016/j.promfg.2018.03.019.
31. Cordos N, Todorut A, Barabas I. Evaluation of the tire pressure influence on the lateral forces that occur between tire and road. IOP Conference Series: Materials Science and Engineering 2017; 252: 012011. DOI: https://doi.org/10.1088/1757-899X/252/1/012011.
32. Abinaya L, Thilagam A, Nivitha MR. Influence of tire pressure on the rutting and fatigue life of bituminous pavement. Sadhana 2022; 47: 71. DOI: https://doi.org/10.1007/s12046-022-01841-2.
33. Arshad AK, Harun MS, Jasmi N, Yaacob S. Effect of heavy vehicles' tyre pressure on flexible pavements. International Journal of Civil Engineering and Technology 2018; 9(9): 1161-1170.
34. Gorzelanczyk P, Wład P, Jurkovic M, Kalina T. Influence of tire pressure on noise road. Transport technic and technology 2021; 17(1). DOI: https://doi.org/10.2478/ttt-2021-0001.
35. Du M, Sun P, Zhou S, Huang H, Zhu J. A Study on the Influence of Tire Speed and Pressure on Measurement Parameters Obtained from High-Speed Tire Uniformity Testing. Vehicles 2020; 2(3): 559-573. DOI: https://doi.org/10.3390/vehicles2030031.
36. Arifin Z, Yoga IN. The Effect of Tire Pressure to Fuel Consumption of G19 Garuda Urban Cars. Journal of Physics: Conference Series 2020; 1700: 012067. DOI: https://doi.org/10.1088/1742-6596/1700/1/012067.
37. Szczucka-Lasota B, Kamińska J, Krzyżewska I. Influence of tire pressure on fuel consumption in trucks with installed tire pressure monitoring system (TPMS). Scientific Journal of Silesian University of Technology. Series Transport 2019; 103: 167-181. DOI: https://doi.org/10.20858/sjsutst.2019.103.13.
38. Ejsmont J, Taryma S, Ronowski G, Świeczko-Żurek B. Influence of load and inflation pressure on the tyre rolling resistance. International Journal of Automotive Technology 2016; 17(2): 237-244. DOI: https://doi.org/10.1007/s12239-016-0023-z.
39. Ejsmont J, Taryma S, Ronowski G, Świeczko-Żurek B. influence of temperature on the tyre rolling resistance. International Journal of Automotive Technology 2018; 19(1): 45-54. DOI: https://doi.org/10.1007/s12239−018−0005−4.
40. Suyabodha A. A Relationship between Tyre Pressure and Rolling Resistance Force under Different Vehicle Speed. MATEC Web of Conferences 2017; 108: 12004. DOI: https://doi.org/10.1051/matecconf/201710812004.
41. Nguyen VT, Nguye VD, Bouteldja M. Estimation of Rolling Resistance, Tire Temperature and Inflation Pressure of Heavy-duty Vehicle. International Journal of Mechanical Engineering and Robotics Research 2022; 11 (4). DOI: https://10.18178/ijmerr.11.4.255-261.
42. Fathi H, El-Sayegh Z, Ghoreishy MHR. Prediction of rolling resistance and wheel force for a passenger car tire: A comparative study on the use of different material models and numerical approaches. Proceedings of the Institution of Mechanical Engineers, Part D 2024. DOI:

https://doi.org/10.1177/09544070241244556